

# Inversion doublets of $3N+N$ cluster structure in excited states of ${}^4\text{He}$

W. Horiuchi<sup>1</sup> and Y. Suzuki<sup>2</sup>

<sup>1</sup>*Graduate School of Science and Technology, Niigata University, Niigata 950-2181, Japan*

<sup>2</sup>*Department of Physics, and Graduate School of Science and Technology, Niigata University, Niigata 950-2181, Japan*

Excited states of  ${}^4\text{He}$  are studied in four-body calculations with explicitly correlated Gaussian bases. All the levels below  $E_x=26$  MeV are reproduced reasonably well using realistic potentials. An analysis is made to show how the  $0_2^+$  state becomes a resonance but those having almost the same structure as this state in different spin-isospin channels are not observed as resonances. The role of tensor force is stressed with a particular attention to the level spacing between the two  $0^-$  states. The calculation of spectroscopic amplitudes, nucleon decay widths, and spin-dipole transition strengths demonstrates that the  $0_2^+$  state and the three lowest-lying negative-parity states with  $0^-$  and  $2^-$  have  ${}^3\text{H}+p$  and  ${}^3\text{He}+n$  cluster configurations, leading to the interpretation that these negative-parity states are the inversion doublet partners of the  $0_2^+$  state.

PACS numbers: 27.10.+h, 21.10.Jx, 21.45.-v, 21.60.De

## I. INTRODUCTION

The competition of particle-hole and cluster excitations is one of the most interesting issues in the structure of light nuclei. They emphasize different aspects of nuclear excitation modes, and often coexist in low-lying spectrum. Both the excitations are usually described in quite different languages, thus defying the reproduction of such a coexistence in a single scheme. In fact some intruder states have remained unresolved even in a large-space calculation based on realistic interactions. For example, the excitation energy of the so-called Hoyle state which is recognized to have large overlap with  $3\alpha$  configuration [1] is predicted too high in the no-core shell model [2]. According to the shell model, negative-parity states should appear first in the excited spectrum of  ${}^{16}\text{O}$ , but they show up just above the first excited  $0^+$  state which is also understandable from  ${}^{12}\text{C}+\alpha$  structure [3].

The  ${}^4\text{He}$  nucleus is a lightest system offering a coexisting spectrum. Its ground state is doubly magic and tightly bound, but its first excited state is not a negative parity but  $0^+$ , similarly to  ${}^{16}\text{O}$ . This state was first conjectured as a breathing mode, but an extensive study has confirmed it as a cluster state of  $3N+N$  ( ${}^3\text{H}+p$  and  ${}^3\text{He}+n$ ) configuration [4]. Accepting this interpretation for this state, we are led to the following questions. Since the  $3N$  and  $N$  clusters having spin  $1/2$  and isospin  $1/2$  move in a relative  $S$  wave, four states may appear which all have basically the same  $3N+N$  configuration but different  $J^\pi T$  with  $0^+0, 1^+0, 0^+1, 1^+1$ . These states may be called quadruplets. The first question we set here is ‘Why do we actually observe only one of them,  $0^+0$ ?’

The second question is concerned with the concept of an inversion doublet which is known in molecular spectroscopy. For a system consisting of asymmetric molecules (clusters), one may expect a partner state of negative parity as in the ammonia molecule. These positive- and negative-parity pairs are called inversion doublets. On the analogy of the molecule we may ask a question ‘What about the possibility of observing

negative-parity partners in which the  $3N$  and  $N$  clusters move in a relative  $P$  wave?’ The negative-parity partners would have  $J^\pi=0^-, 1^-,$  and/or  $2^-$ , which result from the coupling of the spins of the two clusters and the relative orbital angular momentum between them. The centrifugal barrier for the  $P$  wave is more than 3 MeV at the  $3N-N$  relative distance of 4 fm, so that the expected partner states may appear in the region of the excitation energy  $E_x=21-23$  MeV. In fact the  $0^-$  and  $2^-$  states are observed in this region. Traditionally, these states are considered  $s^3p$  shell-model states, but could be better understood from the  $3N+N$  configuration. The ATMS variational calculation seems to suggest this picture for the negative-parity states [5] but no discussion was made on the relationship between them and the  $0_2^+0$  state. According to recent large-space shell-model calculations, these  $0^\pm 0$  states show quite different convergence [6]: Because of its slow convergence, the  $0_2^+0$  state is attributed to a radial excitation.

The purpose of this study is to answer the two questions by performing four-body calculations with realistic potentials. Thus we are mainly interested in the three excited states,  $0^+0$  ( $E_x=20.21$  MeV),  $0^-0$  (21.01 MeV), and  $2^-0$  (21.84 MeV), but also consider other excited states which all have a width larger than 5 MeV. We will not invoke any model ansatz, that is, our calculation is based on neither the shell model nor an RGM calculation [7, 8] which couples  ${}^3\text{H}+p$ ,  ${}^3\text{He}+n$ , and  $d+d$  two-cluster channels, but treat four nucleons equally in an unconstrained configuration space. We will obtain the energies and wave functions of the excited states of  ${}^4\text{He}$  in a basis expansion method. The basis used here is square integrable, so that the excited states are obtained in a bound-state approximation. As we show later, this approximation works fairly well for predicting the three lowest-lying excited states, but it gives only a qualitative prediction for the other broad levels.

Section II gives a brief description of the basis functions used to solve the four-body problem. Section III presents the results of calculation together with some discussions. We show the energy spectrum of  ${}^4\text{He}$  in Sec. III A, dis-

cuss the problem about the quadruplets in Sec. III B and answer the question concerning the inversion doublets in Sec. III C. Section IV draws a conclusion of the present work.

## II. FORMULATION

The Hamiltonian  $H$  for a system of two protons and two neutrons consists of the kinetic energy ( $T$ ) and a nucleon-nucleon potential including the Coulomb potential ( $V_{\text{Coul}}$ ). The center of mass kinetic energy is properly subtracted. A three-body force is ignored as it has a small effect on the spectrum above the  $3N+N$  threshold [9]. We use the G3RS potential [10] and the AV8' potential [11] as the two-nucleon interaction. Both of them contain central ( $V_c$ ), tensor ( $V_t$ ) and spin-orbit ( $V_b$ ) terms. The  $\mathbf{L}^2$  and  $\mathbf{L}\cdot\mathbf{S}$  terms of the G3RS potential are ignored. The ground-state properties of  $d$ ,  ${}^3\text{H}$ ,  ${}^3\text{He}$ , and  ${}^4\text{He}$  given by these potentials are similar to each other [12]. The tensor and spin-orbit forces of the AV8' potential are, however, stronger than those of the G3RS potential, while the central force of the AV8' potential is weaker than the one of the G3RS potential.

A variational solution  $\Psi_{JM_JTM_T}$  for the Schrödinger equation is obtained by taking a linear combination of many basis states, each of which has the following form

$$\begin{aligned} \Phi_{(LS)JM_JTM_T} \\ = \mathcal{A}\{e^{-\frac{1}{2}\tilde{\mathbf{x}}A\mathbf{x}} [[\mathcal{Y}_{L_1}(\tilde{u}_1\mathbf{x})\mathcal{Y}_{L_2}(\tilde{u}_2\mathbf{x})]_L\chi_S]_{JM_J}\eta_{TM_T}\}, \quad (1) \end{aligned}$$

where  $\mathcal{Y}_\ell(\mathbf{r}) = r^\ell Y_\ell(\hat{\mathbf{r}})$  is a solid spherical harmonic. Here  $\mathcal{A}$  is the antisymmetrizer,  $\mathbf{x}$  a column vector whose elements are three relative coordinates ( $\mathbf{x}_1, \mathbf{x}_2, \mathbf{x}_3$ ), and  $A$  is a  $3\times 3$  positive-definite, symmetric matrix whose 6 independent elements are variational parameters. The vectors  $u_1$  and  $u_2$  each contain three elements determining the weightings of the relative coordinates and are used to specify the angular motion of the basis (1). The tilde  $\sim$  stands for the transpose of a column vector, and thus the inner product  $\tilde{u}_1\mathbf{x}$ , which we call a global vector, is a vector in three-dimensional coordinate space. However, the inner product  $\tilde{\mathbf{x}}A\mathbf{x}$  denotes a scalar in three-dimensional space as it is defined by  $\sum_i \mathbf{x}_i \cdot (A\mathbf{x})_i = \sum_{i,j} A_{ij} \mathbf{x}_i \cdot \mathbf{x}_j$ .

The global vector representation for the rotational motion used in Eq. (1) is found to be very useful. A reader is referred to Refs. [12, 13] for more detail. The spin function  $\chi_{SM_S}$  in Eq. (1) is specified in a successive coupling,  $[[[\frac{1}{2}\frac{1}{2}]_{S_{12}}\frac{1}{2}]_{S_{123}}\frac{1}{2}]_{SM_S}$ , and all possible intermediate spins ( $S_{12}, S_{123}$ ) are taken into account in the calculation. The isospin function  $\eta_{TM_T}$  is also treated in exactly the same way as the spin function. We include the following  $(LS)$  values in Eq. (1) to obtain the state with  $J^\pi$  for both

$T=0$  and 1:

$$\begin{aligned} J^\pi & (LS) \\ 0^+ & (00), (22); (11) \\ 1^+ & (01), (21), (22); (10), (11), (12), (32) \\ 0^- & (11); (22) \\ 1^- & (10), (11), (12), (32); (21), (22) \\ 2^- & (11), (12), (31), (32); (20), (21), (22), (42). \end{aligned}$$

Here the semicolon divides a natural parity set from an unnatural parity one. The values of  $L_1, L_2$  in Eq. (1) for a given  $L$  are chosen to be  $L, 0$  for the natural parity and  $L, 1$  for the unnatural parity. Any basis functions with  $L^\pi=0^-$  are not included in the present calculation.

Each basis function differs in the choices of  $A, u_1$ , and  $u_2$ . The exponential part specified by  $A$  is called an explicitly correlated Gaussian. An alternative expression for this part is given using the single-particle coordinate  $\mathbf{r}_i$  as [14]

$$e^{-\frac{1}{2}\tilde{\mathbf{x}}A\mathbf{x}} = \exp\left[-\frac{1}{2}\sum_{i<j}\left(\frac{\mathbf{r}_i - \mathbf{r}_j}{b_{ij}}\right)^2\right]. \quad (2)$$

Specifying the elements of  $A$  using the 6 variables,  $(b_{12}, b_{13}, \dots, b_{34})$ , is convenient for controlling the spatial extension of the system.

## III. RESULTS

### A. Energy spectrum

The accuracy of our solution depends on the basis dimension and the optimization of the variational parameters. The selection of the parameters is performed by the stochastic variational method [14, 15]. As all the states but the ground state are resonances, increasing the basis size unconditionally does not always lead to a solution we are seeking. Namely, if the variational parameters are allowed to reach very far in the spatial region, the energy for the excited state would fall down to the  ${}^3\text{H}+p$  threshold.

Some details of the calculation are given below. The  $b_{ij}$  parameters are restricted to  $0 < b_{ij} < 8$  fm for all the states but the  $0^-1$  state. This choice covers the configuration space large enough to obtain accurate solutions for both the ground and first excited states [12]. Each element of  $u_i$  is allowed to take a value in the interval  $[-1, 1]$  under the constraint that its norm is unity, *i.e.*  $\tilde{u}_i u_i = 1$ . Note that changing the normalization of  $u_i$  does not actually alter the basis function (1) except for its normalization. We found that using 600 basis states of the form given in Eq. (1) (that is, 600 choices of parameters for  $A, u_1, u_2, L, S, S_{12}, S_{123}, T_{12}, T_{123}$ ) enabled us to obtain converged solutions for both the ground and first excited states. See Fig. 1 of Ref. [12]. Solutions for the other states are obtained in the basis dimension of 300.

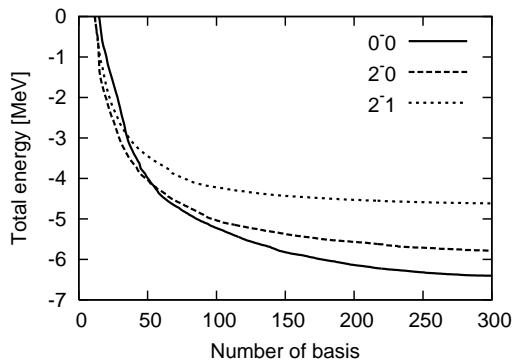


FIG. 1: The energy convergence of the three lowest-lying negative-parity states of  ${}^4\text{He}$  calculated using the G3RS potential.

Figure 1 displays the energy convergence of the three lowest-lying negative-parity states with  $J^\pi T=0^-0$ ,  $2^-0$ , and  $2^-1$  as a function of basis dimension. The energies of these states are considerably stable for the increase of basis functions, though they do not have proper asymptotic behavior characteristic of a resonance. The energies of the other levels are not very accurately obtained. They have a large width, so that we think our calculation gives only an approximate energy. In particular we found that the energy of the  $0^-1$  state, which has a width of about 8 MeV, was not as stable as the other states. We thus obtained its energy by restricting the range of  $b_{ij}$  as  $0 < b_{ij} < 6$  fm.

Figure 2 compares the spectrum of  ${}^4\text{He}$  between theory and experiment. The calculated binding energy of  ${}^3\text{H}$  is 7.73 MeV for G3RS and 7.76 MeV for AV8' [12]. Thus the calculated  ${}^3\text{H}+p$  threshold energy does not agree by

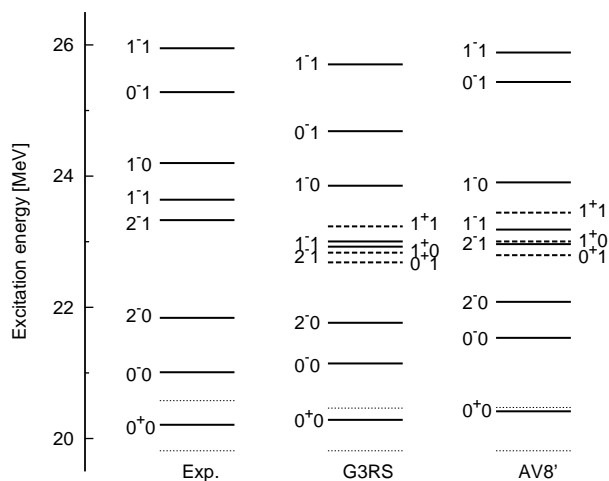


FIG. 2: Energy levels of the excited states of  ${}^4\text{He}$  labeled with  $J^\pi T$ . Three of the quadruplets are drawn by dashed lines. The dotted lines indicate the  ${}^3\text{H}+p$  and  ${}^3\text{He}+n$  thresholds, respectively. Experimental values are taken from Ref. [16].

about 0.7 MeV with the experimental one. The theoretical spectrum in the figure is drawn by shifting the calculated spectrum energies downward so as to adjust this difference of the threshold energy. The theory reproduces the level sequence of the spectrum as a whole and especially the excitation energies of the  $0_2^+0$ ,  $0^-0$ , and  $2^-0$  states very well. The levels above  $E_x=23$  MeV are predicted to be slightly lower than experiment except for the  $0^-1$  level with AV8'. As their widths are all larger than 5 MeV, this discrepancy may be allowable in the bound-state approximation for unbound states. Noteworthy is that the calculation predicts three states with  $0^+1$ ,  $1^+0$ , and  $1^+1$  around  $E_x=23$  MeV, as denoted by dashed lines. These states together with the  $0_2^+0$  state are the quadruplets relevant to the first question. As speculated, they show up in the present calculation, but no such states are observed experimentally.

## B. Quadruplets

To resolve the first problem on the quadruplets, we begin by understanding why only the  $0_2^+0$  state gets considerably lower than the other quadruplet members. As shown in Table I, all the members of the quadruplets consist of about 93%  $L=0$  and 7%  $L=2$  components. These values are almost equal to the corresponding components in  ${}^3\text{H}$  and  ${}^3\text{He}$  [12], consistently with the conjecture that the quadruplets have  $3N+N$  cluster structure with a relative  $S$ -wave motion.

We list in Table II the energy contents of the quadruplet members. The matrix elements of the Hamiltonian  $H$  as well as its every piece are shown in a matrix form. The row and column labels of the  $3\times 3$  matrix correspond to the configuration space with  $L=0, 2$ , and 1. The off-diagonal elements in the lower triangular part of the matrix are added to the corresponding elements in the upper triangular part. We see that the key elements which give only the  $0_2^+0$  state about 3 MeV larger binding energy than the other members are the kinetic energy as well as the tensor force. The kinetic energy contribution from the main channel listed in Table I is found to be about 2 MeV smaller in the  $0_2^+0$  state than in the other states. This is a consequence of the symmetry of the orbital part of the wave function as understood from Wigner's supermultiplet theory [17]. The spin and isospin function

TABLE I: Percentages of ( $LS$ ) components of the quadruplets calculated using the G3RS potential. Unnatural parity components are negligibly small.

	$0_2^+0$	$0^+1$	$1^+0$	$1^+1$
(00)	93.0	93.4	-	-
(01)	-	-	93.3	93.4
(21)	-	-	3.0	3.4
(22)	6.9	6.6	3.7	3.1

TABLE II: Total energy of the quadruplets, given in MeV, and its decomposition into the contributions from the kinetic energy and the different potential pieces. The row and column of each  $3 \times 3$  matrix correspond to the configuration space with  $L=0, 2$ , and 1. The off-diagonal elements in the lower triangular part of the matrix are added to the corresponding elements in the upper triangular part. For example, 4.58,  $-22.65$  and  $-0.00$  in the first row means the energy contribution of  $(L, L')=(0,0)$  channel,  $(0,2)$  and  $(2,0)$  channels and  $(0,1)$  and  $(1,0)$  channels, respectively. The contributions of  $L=3$  are negligible and omitted. The G3RS potential is used.

	$T=0$						$T=1$					
	$0^+$			$1^+$			$0^+$			$1^+$		
$\langle H \rangle$	4.58	-22.65	-0.00	6.48	-21.74	-0.01	6.30	-21.67	-0.00	6.62	-21.31	-0.01
		10.97	-0.29		10.64	-0.16		10.58	-0.12		10.45	-0.15
			0.14			0.08			0.06			0.08
$\langle T \rangle$	29.26	-	-	31.09	-	-	31.45	-	-	31.73	-	-
		10.99	-		10.30	-		10.31	-		10.08	-
			0.15			0.08			0.06			0.08
$\langle V_c \rangle$	-25.07	-	-	-25.00	-	-	-25.54	-	-	-25.50	-	-
		-1.56	-		-1.26	-		-1.28	-		-1.17	-
			-0.01			-0.00			-0.00			-0.00
$\langle V_{\text{Coul}} \rangle$	0.39	-	-	0.39	-	-	0.39	-	-	0.40	-	-
		0.03	-		0.03	-		0.03	-		0.02	-
			0.00			0.00			0.00			0.00
$\langle V_t \rangle$	-	-22.65	-	-	-21.75	-	-	-21.67	-	-	-21.31	-
		1.54	-0.30		1.61	-0.16		1.56	-0.13		1.55	-0.13
			0.01			0.00			0.00			0.00
$\langle V_b \rangle$	-	-	-0.00	-	-	-0.01	-	-	-0.00	-	-	-0.01
		-0.02	0.00		-0.03	0.00		-0.05	0.00		-0.03	0.00
			0.00			0.00			0.00			0.00

of four nucleons contains more number of antisymmetric pairs in  $S=0, T=0$  channel than in other  $ST$  channels, so that the orbital part of the  $0_2^+0$  state is more symmetric with respect to the nucleon-exchange than the other orbital functions. Furthermore, the  $0_2^+0$  state gains about 1 MeV energy compared to the others states, due to the tensor coupling between the  $L=0$  and  $L=2$  components.

Now we discuss whether or not the quadruplets can be observed as resonances in  ${}^3\text{H}+p$  and  ${}^3\text{He}+n$  decay

channels. To this end we calculate a spectroscopic (or reduced width) amplitude (SA) defined as

$$y(r) = \sqrt{\frac{4!}{3!}} \left\langle \left[ \left[ \Psi_{\frac{1}{2}, \frac{1}{2} m_t}(3N) \phi_{\frac{1}{2}, \frac{1}{2} - m_t}(N) \right]_I Y_\ell(\hat{\mathbf{R}}) \right]_{JM_J} \right\rangle \times \frac{\delta(R-r)}{Rr} \left| \Psi_{JM_J T 0}({}^4\text{He}) \right\rangle. \quad (3)$$

Here  $\mathbf{R}$  is the  $3N$ - $N$  relative distance vector,  $\Psi_{1/2, 1/2 m_t}$  the normalized  $3N$  ground-state wave function, and  $\phi_{1/2, 1/2 - m_t}$  is the nucleon spin-isospin function. They are coupled to the channel spin  $I$ . The label  $m_t$  distinguishes either  ${}^3\text{H}+p$  ( $m_t=1/2$ ) or  ${}^3\text{He}+n$  ( $m_t=-1/2$ ) channel. The  $3N$  wave function  $\Psi_{1/2, 1/2 m_t}$  used here is obtained in the calculation using the basis of type (1) with  $(LS)=(0\frac{1}{2})$  and  $(2\frac{3}{2})$  [12]. The component of  $L=1$  is very small (0.05%) and ignored unless otherwise. Figure 3 displays the  ${}^3\text{He}+n$  SA of the quadruplets. The orbital angular momentum between the clusters is set to  $\ell=0$ , and so  $I$  is equal to  $J$ . The  ${}^3\text{H}+p$  SA is virtually the same as the  ${}^3\text{He}+n$  SA (except for the phase). The  $0_2^+0$  state exhibits behavior quite different from the others: Its peak position is 3 fm, outside the  $3N$  radius ( $\sim 2.3$  fm). Moreover, the spectroscopic factor defined as  $\int_0^\infty y^2(r) r^2 dr$  is so large as 1.03. In a sharp contrast to the  $0_2^+0$  state, the SAs of the other quadruplet members show nothing of resonant behavior: The peaks are

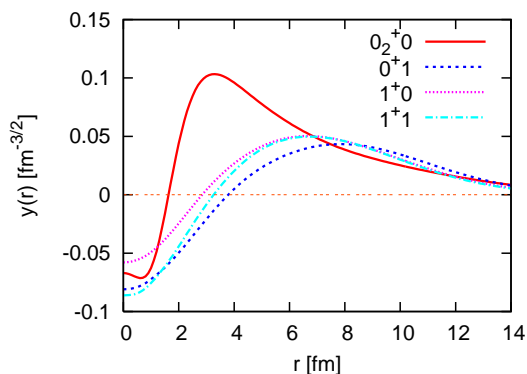


FIG. 3: (Color online) SAs of the quadruplets for the  $S$ -wave  ${}^3\text{He}+n$  decay. The G3RS potential is used.

located extremely far outside the  $3N$  radius, and the  $y^2$  value is small in the inner region. In passing we note that the SA of the ground state has a sharp contrast with that of the  $0_2^+$  state: The peak appears near the origin and the amplitude is confined mostly in the  $3N$  radius.

Since our variational solution is expected to be fairly accurate at least in the inner region, a decay width can be estimated with the formula of  $R$ -matrix type:

$$\Gamma_N = 2P_\ell(kr) \frac{\hbar^2 r}{2\mu} y^2(r), \quad (4)$$

where  $k$  is the wave number given by  $k = \sqrt{2\mu E/\hbar^2}$  with the decay energy  $E$ ,  $\mu$  the reduced mass of the decaying particles, and  $P_\ell$  is the penetrability

$$P_\ell(kr) = \begin{cases} \frac{kr}{F_\ell^2(kr) + G_\ell^2(kr)} & \text{for } {}^3\text{H}+p \\ \frac{kr}{(kr)^2 [j_\ell^2(kr) + n_\ell^2(kr)]} & \text{for } {}^3\text{He}+n \end{cases} \quad (5)$$

which is expressed in terms of either Coulomb wave functions or spherical Bessel functions. The decay width (4) depends on the channel radius  $r$ , but its dependence is found to be mild: The  $\Gamma_p$  value of the  $0_2^+$  state is 0.69, 0.74, 0.67 MeV at  $r=4, 5, 6$  fm, in good agreement with the empirical value of 0.50 MeV [16]. The above analyses all confirm that the  $0_2^+$  state has well-developed  $3N+N$  cluster structure, in accordance with the conclusion of Ref. [4]. Moreover, we conclude that none of the quadruplets except for the  $0_2^+$  state is a physically observable resonance. This conclusion is consistent with the RGM phase-shift analysis which finds no resonance around 23 MeV excitation energy region[8].

As discussed above, all the quadruplet members but the  $0_2^+$  state do not gain energy large enough to come down below the  ${}^3\text{He}+n$  threshold. Only the  $0_2^+$  state shows up between the  ${}^3\text{H}+p$  and  ${}^3\text{He}+n$  thresholds thanks to their Coulomb energy difference. The isospin conservation gives the  $0_2^+$  state an almost equal mixing of the open ( ${}^3\text{H}+p$ ) and closed ( ${}^3\text{He}+n$ ) channels. Both effects of the isospin conservation and the  ${}^3\text{H}+p$  Coulomb barrier make the  $\Gamma_p$  value of the  $0_2^+$  state rather small. This state is thus a good example of a Feshbach resonance [18].

### C. Negative-parity partners of the first excited $0^+$ state

Before coming to the inversion doublet issue, we first comment on the features of the negative-parity states. According to the shell model, the negative-parity states basically arise from the  $s_{1/2}^{-1}p_{3/2}$  or  $s_{1/2}^{-1}p_{1/2}$  particle-hole excitation, which predicts  $J^\pi=0^-, 1^-, 1^-,$  and  $2^-$  for both  $T=0$  and 1. However, a suitable combination of the two  $1^-$  states with  $T=0$  corresponds to the excitation of the center of mass, leaving only one  $1^-$  state with  $T=0$ . Seven negative-parity states observed experimentally below  $E_x=26$  MeV include three states with  $T=0$

TABLE III: Percentage of ( $LS$ ) components of the negative-parity states calculated using the G3RS potential. The natural and unnatural parity channels are separated by the line.

$(LS)$	$T=0$			$T=1$			
	$0^-$	$1^-$	$2^-$	$0^-$	$1_1^-$	$1_2^-$	$2^-$
(10)	-	19.7	-	-	51.0	42.9	-
(11)	95.5	74.2	93.0	96.9	43.0	53.1	93.7
(12)	-	0.8	0.3	-	0.0	0.6	0.2
(31)	-	-	2.9	-	-	-	2.8
(32)	-	3.4	2.0	-	4.3	0.1	1.7
(20)	-	-	0.0	-	-	-	0.0
(21)	-	1.8	0.5	-	1.1	1.5	0.5
(22)	4.5	0.2	1.4	3.1	0.5	1.8	1.1
(42)	-	-	0.0	-	-	-	0.0

and four states with  $T=1$ , which is in agreement with the shell-model prediction. However, this agreement may not necessarily mean that the negative-parity states have shell-model like structure because the present four-body calculation also produces seven negative-parity states, as shown in Fig. 2.

The level sequence is  $0^-, 2^-$ , and  $1^-$  in the order of increasing energy for  $T=0$ , while it is  $2^-, 1^-, 0^-$ , and  $1^-$  for  $T=1$ . Therefore the energy difference between the  $0^-0$  and  $0^-1$  states becomes much larger than the one between the  $1^-0$  and  $1^-1$  states or between the  $2^-0$  and  $2^-1$  states. It is interesting to clarify the mechanism of how this large energy difference is produced compared to the other negative-parity states with the same  $J^\pi$ . Table III lists the percentage analysis of the seven negative-parity states according to their ( $LS$ ) channels. The main component has  $L=1$  as expected from the shell model. The percentages are rather similar between the states with the same  $J^\pi$  but different  $T$  values. The similarity of the percentages is, however, not very clear in the  $1^-$  states because the values are fragmented into the two  $1^-1$  states. The main channel with  $L=1$  itself has a contribution from the tensor force but also gets a contribution from the other channels through the tensor coupling. For example, the tensor force couples the natural parity channel (11) with the unnatural parity channel (22).

Table IV lists the energy content contributed from each piece of the Hamiltonian. Most striking is a different contribution of the tensor force. Compared to the  $0^-1$  state, the  $0^-0$  state gains about 9 MeV energy from the tensor force, while the contribution of the central force to the energy gain is only about its half. The energy contents given by the AV8' potential are similar to those of the G3RS potential: The gain by the tensor force is even larger, about 12 MeV and the central force gives 3 MeV difference. The tensor force is most attractive in the triplet even  $NN$  state, and it can be taken advantage of by having more number of antisymmetric  $NN$  pairs in the isospin space. The number of such antisymmetric pairs is counted from  $\langle \eta_{TM_T} | \sum_{i<j} (1 - \tau_i \cdot \tau_j) / 4 | \eta_{TM_T} \rangle$ ,

TABLE IV: Energy contents, given in MeV, of the negative-parity states. The G3RS potential is used.

	$0^-0$	$0^-1$	$2^-0$	$2^-1$	$1^-0$	$1^-1$	$1^-2$
$\langle H \rangle$	-6.40	-2.86	-5.78	-4.62	-3.69	-4.54	-1.84
$\langle T \rangle$	48.38	39.10	41.08	40.25	37.72	39.30	32.48
$\langle V_c \rangle$	-28.92	-24.79	-25.71	-25.82	-23.50	-25.14	-22.01
$\langle V_{\text{Coul}} \rangle$	0.48	0.44	0.42	0.43	0.40	0.43	0.42
$\langle V_t \rangle$	-26.63	-17.75	-21.39	-19.30	-18.32	-19.13	-12.67
$\langle V_b \rangle$	0.29	0.14	-0.18	-0.18	0.006	0.005	-0.06

which is  $[A(A+2) - 4T(T+1)]/8$  for  $A$ -nucleon system. Thus the  $0^-0$  state gains more attraction than the  $0^-1$  state through both the (11)-(11) diagonal and (11)-(22) off-diagonal contributions [12]. If the unnatural parity basis were not included in the calculation, the  $\langle V_t \rangle$  value of the  $0^-0$  state would decrease to about half [12] and the  $0^-0$  state would lose significant energy. The role of the tensor force in lowering the energy of the  $0^-0$  state was discussed many years ago [5, 19]. To be exact, the energy difference between the two states is actually a combined effect of the tensor, kinetic and central terms.

Now we discuss the characteristics of the low-lying negative-parity states from the viewpoint of clustering. In Fig. 4 we display the  ${}^3\text{He}+n$  SAs calculated from the three lowest-lying negative-parity states with  $0^-0$ ,  $2^-0$ , and  $2^-1$ . The  $\ell$  value for the  ${}^3\text{He}-n$  relative motion is 1, and the channel spin  $I$  is 1. As expected, each of the three curves shows behavior suggesting  $3N+N$  cluster structure: The peaks are centered around 2 fm near the  $3N$  surface, and the  $y^2$  values are fairly large in the inner region. It is the centrifugal potential that makes the peak positions closer to the origin than that of the first excited  $0^+0$  state. The  $3N+N$  spectroscopic factors are considerably large: 0.58, 0.52, and 0.53 for the  $0^-0$ ,  $2^-0$ , and  $2^-1$  states. We estimate the nucleon width. Its channel-radius dependence is again mild, so we choose  $r=5$  fm. The results for  $(\Gamma, \Gamma_p/\Gamma)$ , where  $\Gamma$  is the total

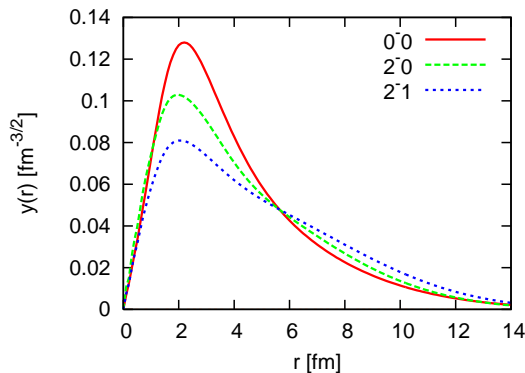


FIG. 4: (Color online) SAs of the three lowest-lying negative-parity states for the  $P$ -wave  ${}^3\text{He}+n$  decay with  $I=1$ . The G3RS potential is used.

width in MeV, are (0.61, 0.72), (1.14, 0.58), and (1.85, 0.53) for  $0^-0$ ,  $2^-0$ , and  $2^-1$ , respectively. These values are compared to those extracted from the  $R$ -matrix analysis [16], (0.84, 0.76), (2.01, 0.63), and (5.01, 0.53). The theory predicts the width of the  $0^-0$  state very well, and gives about half of the width for the other states. Though the degree of clustering is somewhat reduced in the negative-parity states compared to the  $0_2^+$  case, the analysis of SA and decay width supports our conjecture that the  $0^-0$  and  $2^-0$  states as well as the  $2^-1$  state constitute inversion-doublet partners of the first excited  $0^+$  state. The RGM phase-shift analysis of  ${}^3\text{H}+p$  scatterings [8] supports the  $P$ -wave resonance interpretation for these negative-parity states. The SAs of the  $1^-$  states around  $E_x=24$  MeV show some degree of  $3N+N$  cluster structure, though their amplitudes are considerably small compared to the  $0^-0$  and  $2^-0$  states in particular.

An inversion doublet picture in nuclei was first proposed to understand the low-lying positive- and negative-parity rotation bands in  ${}^{16}\text{O}$  and  ${}^{20}\text{Ne}$  from an  $\alpha$ -core molecular structure [20]. The appearance of positive- and negative-parity partners is a natural consequence of the underlying intrinsic structure dominated by the existence of asymmetric clusters. We have shown that the three lowest-lying negative-parity states have a significant component of  $3N$  and  $N$  clusters whose relative motion is in  $P$ -wave. It is important to realize that this result is obtained in the calculation which assumes no cluster ansatz for the wave functions. A physical reason for the appearance of the inversion doublet partners is that they are located near the  $3N+N$  threshold.

Very unique in the inversion doublets in  ${}^4\text{He}$  is that the  $3N$  and  $N$  clusters have both  $J=1/2$ , and the channel spin  $I$  is different in the doublets: It is 0 for  $0_2^+0$  and 1 for  $0^-0$ ,  $2^-0$ , and  $2^-1$ . The negative-parity partners with  $T=0$  should thus be characterized by the transition of an isoscalar spin-dipole operator,  $\mathcal{O}_{\lambda\nu} = \sum_{i=1}^4 [\boldsymbol{\sigma}_i \times (\mathbf{r}_i - \mathbf{x}_4)]_{\lambda\nu}$ , where  $\mathbf{x}_4$  is the center of mass of  ${}^4\text{He}$ . Note that  $\mathbf{r}_i - \mathbf{x}_4$  is proportional to the distance vector between nucleon  $i$  and the center of mass of the other three nucleons. The transition strength to the  $0_2^+0$  state,  $|\langle 0_2^+0 | \mathcal{O}_0 | 0^-0 \rangle|^2$ , is  $11.9 \text{ fm}^2$ , which is 6.9 times larger than that to the ground state. Moreover, the strength  $|\langle 0_2^+0 | \mathcal{O}_0 | 0^-0 \rangle|^2$  between the doublet partners occupies 58% of the ‘‘sum rule’’  $\sum_n |\langle 0_n^+0 | \mathcal{O}_0 | 0^-0 \rangle|^2$ , where  $n$  takes all 600 eigen-

states with  $0^+0$ . A similar enhancement occurs for the  $2^-0$  state as well. The value  $|\langle 0_2^+0 || \mathcal{O}_2 || 2^-0 \rangle|^2/5$  is  $21.7\text{fm}^2$ , which is about 24 times larger than the one to the ground state, and it corresponds to 78% of the total sum  $\sum_n |\langle 0_n^+0 || \mathcal{O}_2 || 2^-0 \rangle|^2/5$ .

For the transition between the  $2^-1$  and  $0_2^+0$  states, an isovector spin-dipole operator,  $\mathcal{O}_{\lambda\nu,10} = \sum_{i=1}^4 [\boldsymbol{\sigma}_i \times (\mathbf{r}_i - \mathbf{x}_4)]_{\lambda\nu} \tau_{3i}$ , must be considered. The transition strength  $|\langle 0_2^+0 || \mathcal{O}_{2,1} || 2^-1 \rangle|^2/15$  is  $17.4\text{fm}^2$ , which is 16 times larger than that to the ground state, where the triple bar  $|||$  indicates that the reduced matrix element is taken in both the angular momentum and isospin spaces. This strength between the  $2^-1$  and  $0_2^+0$  states occupies 87% of the total strength  $\sum_n |\langle 0_n^+0 || \mathcal{O}_{2,1} || 2^-1 \rangle|^2/15$ .

The high collectivity of the spin-dipole strength strongly indicates that the intrinsic structure of the negative-parity states,  $0^-0$ ,  $2^-0$ , and  $2^-1$ , is similar to that of the first excited  $0_2^+0$  state.

#### IV. CONCLUSION

A rich spectrum of  $^4\text{He}$  comprising the coexisting levels has been reproduced in a single scheme without recourse to a specific model assumption. This has offered a good example of demonstrating the power of the global vector representation for the angular part of few-body systems.

We have explained how only the  $0_2^+$  state is observed as a resonance among the quadruplets by examining the symmetry property of the wave functions as well as the role of the tensor force. Analyzing the spectroscopic amplitudes, nucleon decay widths and spin-dipole transition probabilities, we have confirmed that both the  $0_2^+$  and negative-parity states with  $0^-0$ ,  $2^-0$ , and  $2^-1$  are dominated by the  $3N+N$  cluster structure and that these negative-parity states can be understood as the inversion doublet partners of the  $0_2^+$  state in a unified way. We have shown that the tensor force plays a vital role to produce the level spacing between the  $0^-$  states with  $T=0$  and 1 through the coupling between the main channel with  $L=1$  and the unnatural-parity channel with  $L=2$ . A study of  $^{16}\text{O}$  in the scheme of  $^{12}\text{C}$ +four nucleons will be interesting as its spectrum has some similarity to that of  $^4\text{He}$ .

This work was in part supported by a Grant for Promotion of Niigata University Research Projects (2005-2007), and a Grant-in Aid for Scientific Research for Young Scientists (No.19-3978). W.H. is a JSPS Research Fellow for Young Scientists. Y.S. thanks the JSPS core-to-core program (Exotic Femo Systems) and the Institute for Nuclear Theory at the University of Washington for the support which enabled him to have useful communications in the INT Workshop on Correlations in Nuclei, November, 2007.

- 
- [1] M. Chernykh, H. Feldmeier, T. Neff, P. von Neumann-Cosel, and A. Richter, Phys. Rev. Lett. **98**, 032501 (2007), and see also references therein.
  - [2] P. Navrátil, J. P. Vary, and B. R. Barrett, Phys. Rev. Lett. **84**, 5728 (2000).
  - [3] Y. Suzuki, Prog. Theor. Phys. **55**, 1751 (1976); *ibid.* **56**, 111 (1976).
  - [4] E. Hiyama, B. F. Gibson, and M. Kamimura, Phys. Rev. C **70**, 031001(R) (2004).
  - [5] M. Sakai, Y. Akaishi, and H. Tanaka, Prog. Theor. Phys. Suppl. **56**, 108 (1974).
  - [6] P. Navrátil and B. R. Barrett, Phys. Rev. C **59**, 1906 (1999); *ibid.* **54**, 2986 (1996).
  - [7] A. Cs6t6 and G. M. Hale, Phys. Rev. C **55**, 2366 (1997).
  - [8] H. M. Hofmann and G. M. Hale, Nucl. Phys. **A613**, 69 (1997); Phys. Rev. C **77**, 044002 (2008).
  - [9] J. Carlson, V. R. Pandharipande, and R. B. Wiringa, Nucl. Phys. **A424**, 47 (1984).
  - [10] R. Tamagaki, Prog. Theor. Phys. **39**, 91 (1968).
  - [11] R. B. Wiringa, V. G. J. Stoks, and R. Schiavilla, Phys. Rev. C **51**, 38 (1995).
  - [12] Y. Suzuki, W. Horiuchi, M. Orabi, and K. Arai, nucl-th/0804.0067. to appear in Few-Body Systems.
  - [13] Y. Suzuki, J. Usukura, and K. Varga, J. Phys. B **31**, 31 (1998); K. Varga, Y. Suzuki, and J. Usukura, Few-Body Systems **24**, 81 (1998).
  - [14] Y. Suzuki and K. Varga, *Stochastic Variational Approach to Quantum-Mechanical Few-Body Problems*, Lecture notes in physics, Vol. m54 (Springer, Berlin, 1998).
  - [15] K. Varga and Y. Suzuki, Phys. Rev. C **52**, 2885 (1995).
  - [16] D. R. Tilley, H. R. Weller, and G. M. Hale, Nucl. Phys. **A541**, 1 (1992).
  - [17] E. Wigner, Phys. Rev. **51**, 106 (1937).
  - [18] H. Feshbach, Ann. Phys. (N.Y.) **5**, 357 (1958); *ibid.* **19**, 287 (1962).
  - [19] B. R. Barrett, Phys. Rev. **154**, 955 (1967).
  - [20] H. Horiuchi and K. Ikeda, Prog. Theor. Phys. **40**, 277 (1968).